

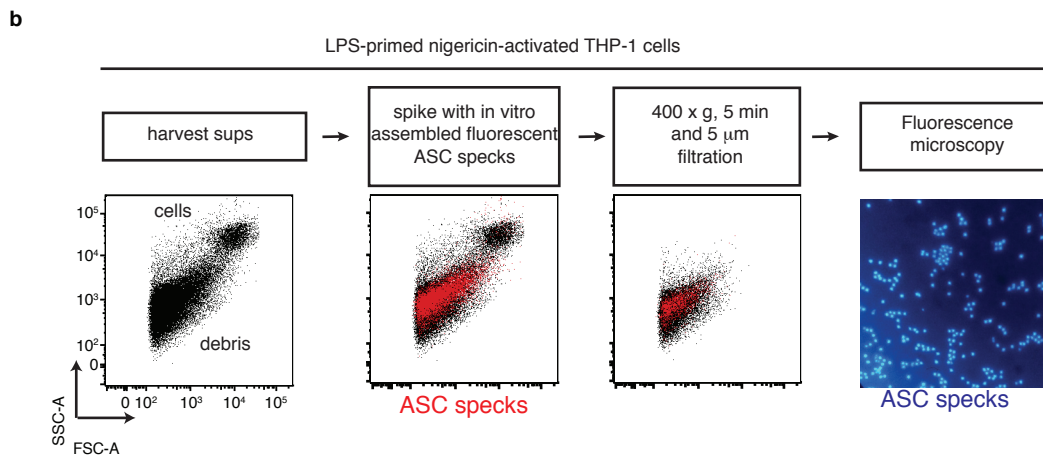
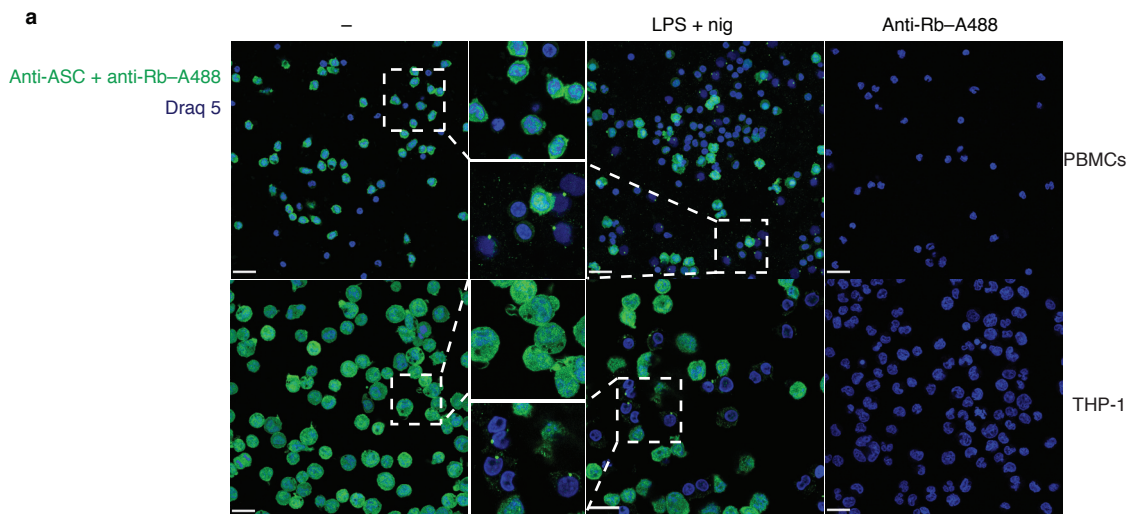
Supplementary Figures

Nature Immunology
NI-A19357A-Z

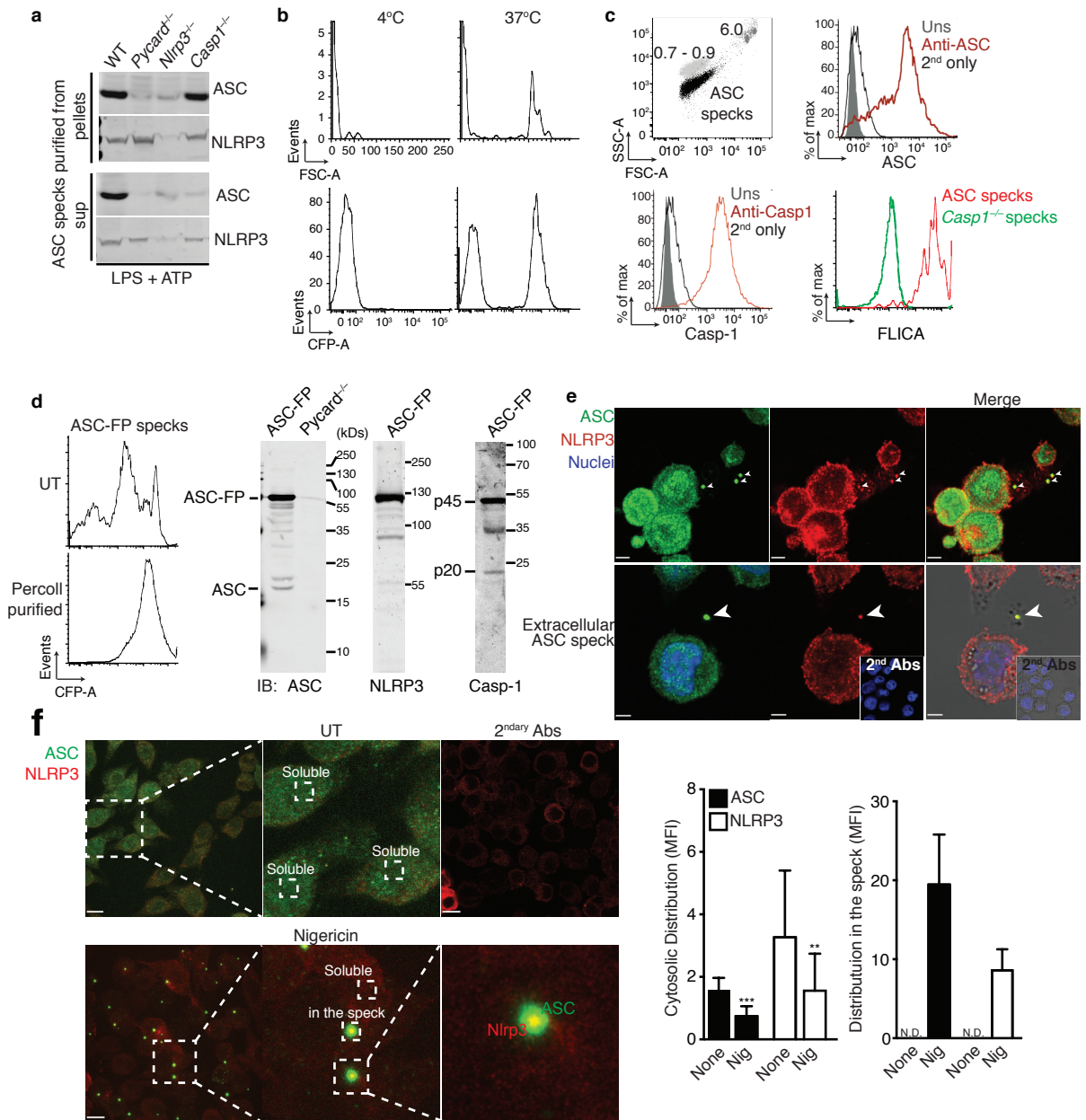
ASC has extracellular and prionoid activities that propagate inflammation

Bernardo S. Franklin¹, Lukas Bossaller^{2,3}, Dominic De Nardo¹, Jacqueline M. Ratter¹, Andrea Stutz¹, Gudrun Engels¹, Christoph Brenker⁵, Mark Nordhoff⁵, Sandra Regina Mirandola⁵, Ashraf Al-Amoudi⁵, Matthew Mangan^{1,5}, Sebastian Zimmer⁴, Brian Monks^{1,3}, Martin Fricke², Reinhold E. Schmidt², Terje Espevik⁶, Bernadette Jones⁷, Andrew G. Jarnicki⁷, Philip M. Hansbro⁷, Patricia Busto³, Ann Marshak-Rothstein³, Simone Hornemann⁸, Adriano Aguzzi⁸, Wolfgang Kastenmüller⁹ and Eicke Latz^{1,3,5,6}

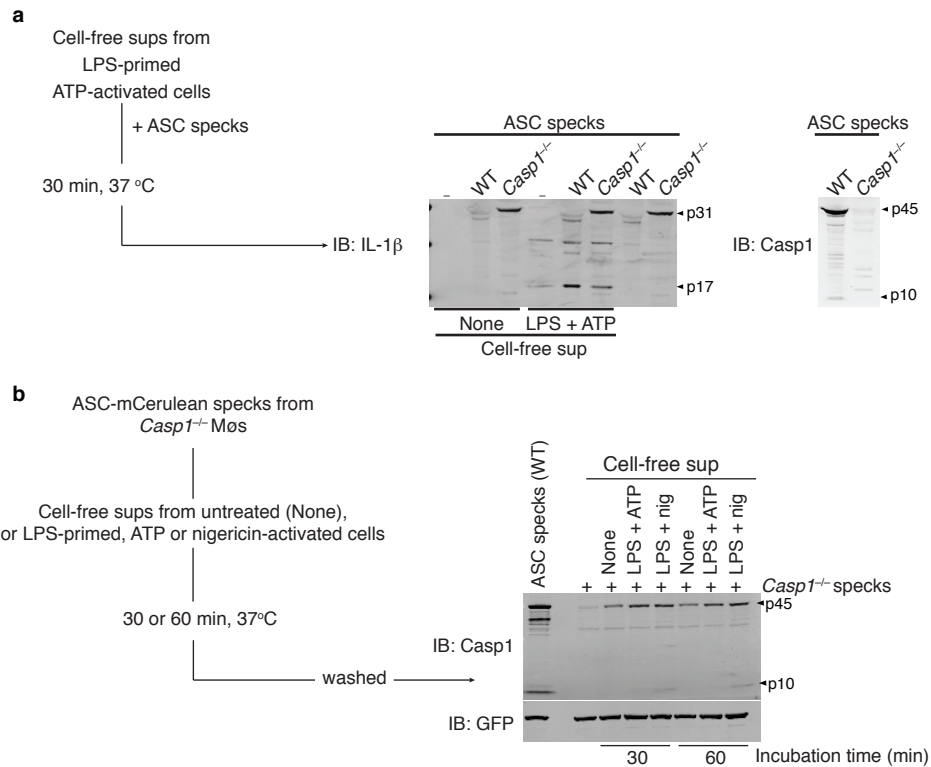
Corresponding Author: Eicke Latz, MD PhD, Institute of Innate Immunity, Biomedical Center, 1G008, University Hospitals, University of Bonn, Sigmund-Freud-Str. 25, 53127 Bonn, Germany, Phone: + 49 (228) 287 51223, Fax: + 49 (228) 287 51221, e-mail: eicke.latz@uni-bonn.de



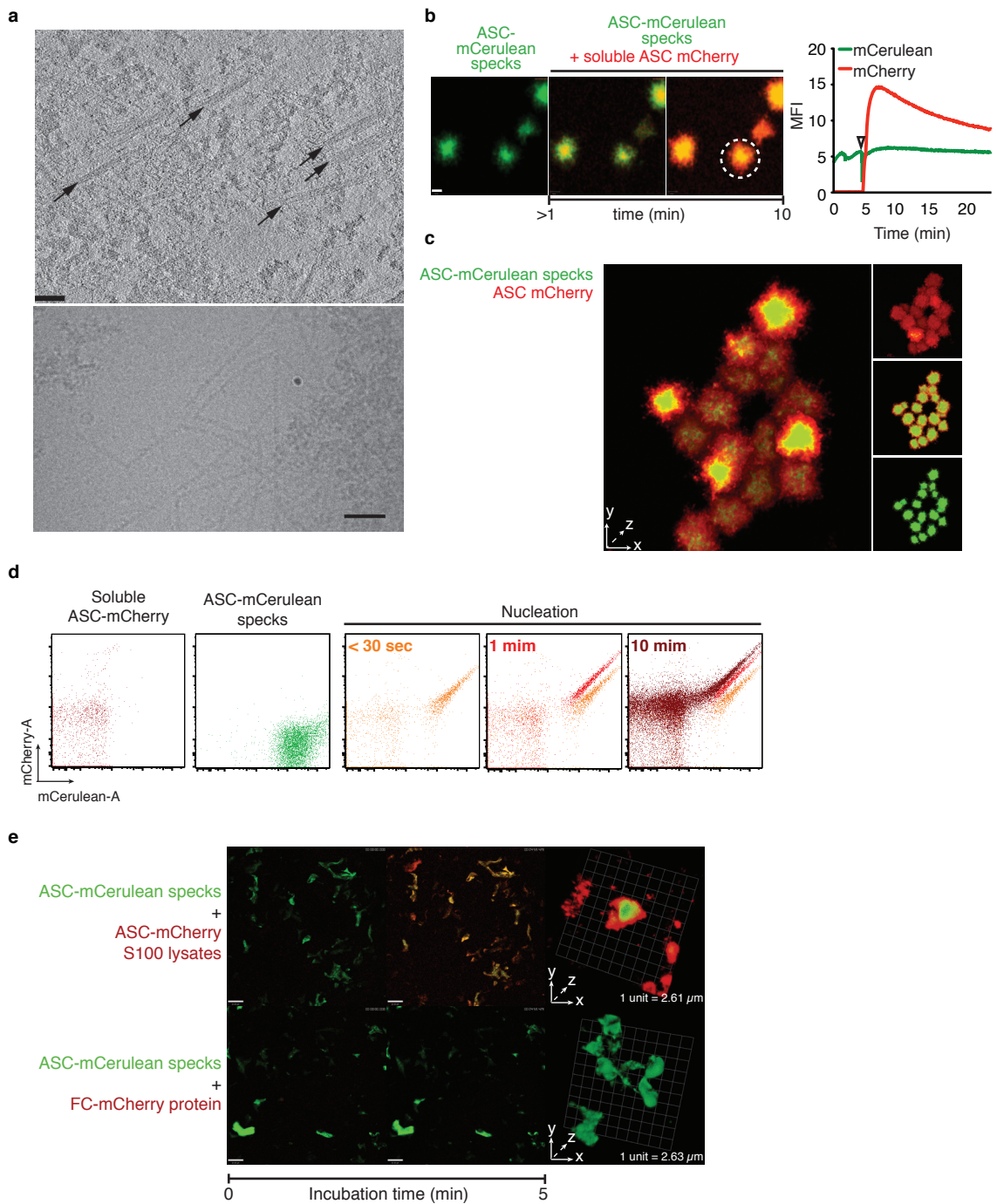
Supplementary Fig 1 ASC forms speck like clusters in different cells. **(a)** Confocal imaging of unstimulated (–) or LPS-primed (200 pg/ml), nigericin-activated (10 μ M) human PBMCs (upper panel) or THP-1 monocytes (LPS 1 μ g/ml, nigericin 10 μ M, lower panel). Scale bars: 22 μ m. **(b)** Flow charge and flow cytometry analysis and fluorescence imaging of ASC-mCerulean specks that were spiked into supernatants of LPS-primed (1 μ g/ml), nigericin-activated (10 μ M) THP-1 monocytes. Data is representative of two independent experiments.



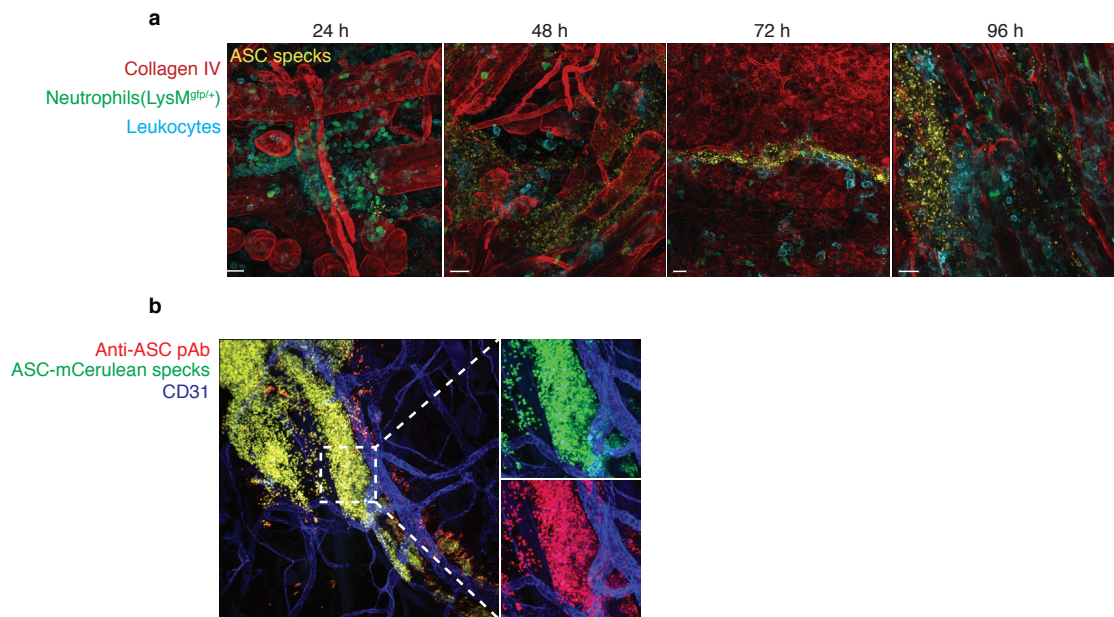
Supplementary Fig 2 (a) Immunoblot of ASC and NLRP3 in ASC specks purified from cell-free supernatants or from whole cell lysates of LPS-primed, ATP activated Wt, *Pycard*^{-/-}, *Casp1*^{-/-} or *Nlrp3*^{-/-} iMøs. (b) Flow cytometry analysis showing *in vitro* assembly of ASC-mCerulean specks from cytosolic lysates (S100) of untreated ASC-mCerulean expressing cells. (c) Flow cytometry analysis of *in vitro*-assembled ASC specks prepared as in b, that were left unstained (Uns) or stained with anti-ASC or anti-Caspase1 Abs followed by staining with A488-directly conjugated secondary Abs. Samples were also stained with the caspase-1 inhibitor z-YVAD-FMK-FITC and compared to ASC specks generated from *Casp1*^{-/-} iMøs. Beads with defined sizes (μm) were used as reference. (d) Flow cytometry analysis showing the purification with a 50% Percoll cushion and immunoblot for ASC, NLRP3 and Caspase-1 in *in vitro*-assembled ASC-mCerulean specks prepared as in b. (e) Confocal imaging of LPS-primed and nigericin-activated WT THP-1 monocytes. Cells were fixed and stained with anti-ASC or anti-NLRP3 Abs coupled to fluorochrome-conjugated secondary Abs. Arrows show intra- and extracellular specks containing both endogenous ASC and NLRP3 proteins. Scale bar: 3.2 μm . (f) Confocal imaging of LPS-primed NLRP3-mCitrine expressing iMøs left untreated (UT) or activated with nigericin (10 μM). Cells were fixed and stained with anti-ASC Abs followed by staining with fluorescence-conjugated secondary Abs. The mean fluorescence intensity (MFI) of ASC or NLRP3 was compared in the cytosol (soluble) and on the specks. Data are from one representative out of two (a-f) independent experiments.



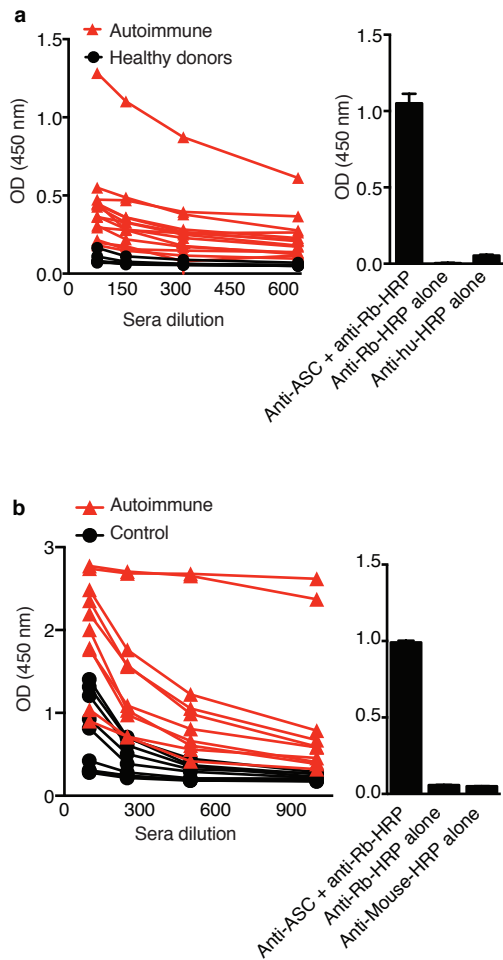
Supplementary Fig 3 ASC specks recruit pro-caspase-1 from cell-free supernatants. (a) Immunoblot for IL-1 β and Caspase-1 in cell-free supernatants from untreated or LPS-primed (500 ng/ml, 3h), ATP activated (2.5 mM) iM ϕ s before and after addition of fluorescent recombinant ASC-mCerulean specks generated from WT or Casp1^{-/-} iM ϕ s. (b) Immunoblot for Caspase-1 and GFP in recombinant ASC-mCerulean specks from WT or Casp1^{-/-} iM ϕ s that were incubated with cell-free supernatants of unstimulated (None), or LPS-primed and ATP, or nigericin-activated iM ϕ s. Data are from one representative of two independent experiments.



Supplementary Fig 4 ASC has prionoid features (a) Cryo-EM of *in vitro*-assembled ASC-mCerulean specks. Scale bars: 100 nm and 200 nm. (b) Time-lapse confocal imaging of the *in vitro* nucleation of soluble ASC-mCherry (red) by ASC-mCerulean specks (green). Scale bar: 4.4 μm . Graph shows mean fluorescence intensity over time of ASC-mCerulean specks after addition of soluble ASC-mCherry. (c) Rendered 3D confocal image of z-stack sections of ASC-mCerulean specks after incubation with soluble ASC-mCherry. (d) Flow cytometry of pre-assembled ASC-mCerulean specks incubated with soluble ASC-mCherry for the indicated time. (e) Confocal imaging of the nucleation of soluble ASC-mCherry, or FC-mCherry protein by ASC-mCerulean specks. Images were recorded every 30 seconds at 63X magnification. Data are from one representative of two (a,d,e) or three (b,c) independent experiments.



Supplementary Fig 5 ASC specks are resistant to proteases *in vivo* (a) *Ex vivo* confocal imaging of whole mount staining of the ears of LysM^{gfp/+} transgenic reporter mice at 24, 48, 72 or 96 hours post injection of 1 μ g of ASC-mCerulean specks in 10 μ l of PBS. (b) *Ex vivo* confocal imaging of subcapsular sinus macrophages of popliteal draining LNs from LysM^{gfp/+} mice injected with 2.5 μ g of ASC-mCerulean specks and re-injected 4 hours later via the same route with PE-labeled anti-ASC Abs. Scale bars: 20 μ m. Data are from a representative out of two independent experiments.



Supplementary Fig 6 Autoimmune sera contains anti-ASC speck Abs (a) ELISA of anti-ASC specks Abs in sera from autoimmune patients (n = 14), or healthy donors (n = 7). (b) ELISA of anti-ASC specks Abs in sera from autoimmune (n = 10), or control (n = 10) mice. ELISA plates were coated with 50 μ g/ml of ASC specks or PBS. Anti-ASC specks Abs in sera were detected with specific anti-human or anti-mouse HRP conjugated secondary Abs. The absorbance (OD) at 450 nm was normalized against the OD obtained in wells coated with PBS and assayed with anti-human or mouse-HRP Abs. The reactivity of secondary Abs against ASC specks without human or mouse sera is shown.